GPS Solutions (2020) 24:24
https://doi.org/10.1007/s10291-019-0930-3

ORIGINAL ARTICLE

Galileo PPP rapid ambiguity resolution with five-frequency observations

Xingxing Li[1] · Gege Liu[1] · Xin Li[1] · Feng Zhou[2] · Guolong Feng[1] · Yongqiang Yuan[1] · Keke Zhang[1]

Received: 24 June 2019 / Accepted: 2 November 2019 / Published online: 9 December 2019
© Springer-Verlag GmbH Germany, part of Springer Nature 2019

Abstract

Galileo, transmitting signals on the five frequencies E1, E5a, E5b, E5 and E6, has completed the fundamental constellation with 26 satellites and now can provide the global positioning service independently. Multi-frequency (triple-frequency or above) signals allow a variety of combinations on different frequencies, which has the potential to improve the performance of the precise point positioning (PPP) ambiguity resolution (AR). We developed a multi-frequency PPP AR method to make use of the Galileo five-frequency observations. The stable multi-frequency uncalibrated phase delay (UPD) products of Galileo were estimated first. It is interesting to find that the extra-wide-lane (EWL) UPDs on the E5a/E5b, E5a/E5 and E5/E5b combined frequencies are very close to zero. With the obtained UPD products, the Galileo triple-, quad- and five-frequency PPP AR was conducted. Triple-frequency PPP AR with different frequency combinations can improve the positioning accuracy of 30 min by 36.6–86.8% compared with float solutions, and 2.3–62.5% compared with dual-frequency PPP AR. Among the five types of frequency combinations, the triple-frequency PPP AR on E1/E5/E6 frequencies shows the best positioning performance with the averaged convergence time shortened to 16.9 min. Furthermore, the averaged convergence time is 15.3 min and 15.0 min for quad- and five-frequency PPP AR, respectively. Compared with the time to first fix (TTFF) of 19.9 min for narrow-lane ambiguity resolution with dual-frequency observations, the TTFF is only shortened by about 1 min with multi-frequency observations. It is beneficial that the EWL and wide-lane (WL) ambiguities can be fixed to integers instantaneously, and the decimeter-level positioning accuracy can be achieved within 0.5 min by utilizing triple-/quad-/five-frequency PPP wide-lane AR (WAR). Moreover, the positioning accuracy of the first epoch derived from Galileo five-frequency PPP WAR is (0.112, 0.144, 0.641) m in the east, north and up components, which has an improvement of 2.1–42.0% compared to triple-/quad-frequency PPP WAR.

Keywords Galileo · Precise point positioning · Multi-frequency observations · Uncalibrated phase delay · Ambiguity resolution · Instantaneous decimeter-level positioning

Introduction

Precise point positioning (PPP) technique enables high-precision positioning on a global scale with only a single receiver and has been demonstrated as a powerful tool in geodetic and geodynamic applications (Malys and Jensen 1990; Zumberge et al. 1997). In recent years, PPP ambiguity resolution (AR) became a highlight topic in the Global Navigation Satellite System (GNSS) community. A number of researches indicate that the initialization process, as well as the position estimate, can be noticeably improved once the ambiguity was fixed correctly (Collins et al. 2008; Zhang et al. 2013).

The European system Galileo has been under development through the collaboration of the European Commission (EC) and the European Space Agency (ESA), and the full constellation will comprise 24 satellites plus at most 6 spares in three orbital planes, expected to be realized by 2020 (Zaminpardaz and Teunissen 2017). As of June 2019, the Galileo has presently 26 satellites in orbit, of which 24 satellites provide healthy signals and valid navigation messages. Galileo satellites transmit permanently three independent signals, named E1, E5 and E6. The E5 signal is

✉ Xin Li
lixinsgg@whu.edu.cn

[1] School of Geodesy and Geomatics, Wuhan University, 129 Luoyu Road, Wuhan 430079, China

[2] College of Geomatics, Shandong University of Science and Technology, Qingdao 266590, China

further sub-divided into signals denoted E5a and E5b (https://gssc.esa.int/navipedia/index.php/Galileo_Signal_Plan). Thus, the Galileo system is capable of transmitting signals on five frequencies centered at E1 (1575.42 MHz), E5a (1176.45 MHz), E5b (1207.14 MHz), E5 (1191.795 MHz) and E6 (1278.75 MHz) for commercial and civilian use (Wang et al. 2018).

With the availability of multi-frequency signals, the performance of Galileo PPP, especially PPP AR, is expected to be further improved. To make use of multi-frequency observations, researchers proposed a variety of triple-frequency PPP models (Henkel et al. 2008; Deo and El-Mowafy 2016). In particular, the new bias called inter-frequency clock bias (IFCB) should be taken into account when processing triple-frequency PPP due to the inconsistency of the observations used for clock estimation and precise positioning. Note that the IFCB only exists in the GPS Block IIF satellites and BDS-2 satellites. For new generation systems, including Galileo, BDS-3 and QZSS, the marginal IFCB variations can be neglected (Montenbruck et al. 2013; Cai et al. 2016; Pan et al. 2017). Compared with the dual-frequency model, a faster convergence and higher positioning accuracy was achieved by triple-frequency PPP AR. Geng and Bock (2013) proposed a method of GPS triple-frequency PPP ambiguity resolution solving the L2/L5 extra-wide-lane (EWL) ambiguity to enable rapid convergences in real-time PPP fixed solutions, based on the simulate observations. Gu et al. (2015) focused on exploiting the contribution of undifferenced (UD) ambiguity resolution to triple-frequency PPP with only EWL and wide-lane (WL) ambiguities fixed to integers. Li et al. (2019) achieved BDS-only, Galileo-only and BDS + Galileo triple-frequency PPP AR in static and kinematic modes. Results show that the triple-frequency PPP fixed solutions present slightly better performance than the dual-frequency PPP fixed solutions in terms of time to the first fix (TTFF) and positioning accuracy, especially for the Galileo-only and BDS + Galileo solutions.

We evaluate and compare the performance of Galileo triple-frequency PPP ambiguity resolution using five types of frequency combinations. For the first time, the quad- and five-frequency PPP AR is performed and assessed. Uncalibrated phase delay (UPD) products are estimated based on observations from 134 International GNSS Service (IGS) stations. With precise and reliable UPD products, the Galileo triple-/quad-/five-frequency PPP AR is achieved and the performance in terms of TTFF, convergence time and positioning accuracy are assessed.

After this introduction, the UPD estimation and multi-frequency PPP AR model are introduced. Then, observation data and the Galileo signal quality are described and analyzed, respectively. After that, the stability of Galileo UPDs is evaluated. Thereafter, the performance of Galileo triple-frequency PPP AR with five types of frequency combinations is investigated and multi-frequency PPP AR are also illustrated and compared. Moreover, instantaneous decimeter-level positioning with multi-frequency PPP wide-lane ambiguity resolution (WAR) is achieved. Finally, the conclusions and perspectives are provided.

Methods

We begin with the basic observation equations for Galileo signals. Then, a detailed description for extra-wide-lane, wide-lane and narrow-lane (NL) UPD estimation is given. Based on Galileo's five-frequency observations, the multi-frequency PPP AR model is also developed.

UPD estimation

The observations of code P and carrier phase L between a Galileo satellite s and receiver r at frequency n can be expressed as followed (Li et al. 2015),

$$P^s_{r,n} = \rho^s_r + c(t_r - t^s) + \gamma_n \cdot I^s_{r,1} + T^s_r + c(b_{r,n} - b^s_n) + e^s_{r,n} \quad (1)$$

$$L^s_{r,n} = \rho^s_r + c(t_r - t^s) - \gamma_n \cdot I^s_{r,1} + T^s_r + \lambda_n \cdot (B_{r,n} - B^s_n) + \lambda_n \cdot N^s_{r,n} + \varepsilon^s_{r,n} \quad (2)$$

where ρ^s_r is the geometric distance between the phase centers of receiver and satellite (m), c is the speed of light in the vacuum (m/s), t_r and t^s are receiver and satellite clock offsets, respectively (s), $I^s_{r,1}$ is the slant ionospheric delay on the E1 frequency (m), γ_n is the frequency-dependent multiplier factor, which can be expressed as $\gamma_n = f_1^2 / f_n^2$, T^s_r denotes the tropospheric delay (m), λ_n is the wavelength of the phase measurement at frequency n (m), $b_{r,n}$ and b^s_n denote frequency-dependent code observation hardware delays for receivers and satellites, respectively (s), $B_{r,n}$ and B^s_n are the phase delays at receiver and satellite sides, respectively (cycles), $N^s_{r,n}$ is the integer phase ambiguity (cycles), and $e^s_{r,n}$ and $\varepsilon^s_{r,n}$ are the sum of noise and multipath error for code and phase observations, respectively (m). In addition, the receiver and satellite antenna phase center offsets (PCOs) and variations (PCVs), relativistic effects, slant hydrostatic delay, tidal loadings, Sagnac effect, and phase wind-up have been corrected with the existing models (Kouba 2009). Precise clock and orbit products generated by GeoForschungsZentrum (GFZ) are used.

To conduct the Galileo multi-frequency PPP AR, the uncalibrated phase delay products, including extra-wide-lane, wide-lane and narrow-lane UPDs, should be estimated first based on five-frequency observations. The EWL and WL ambiguities are commonly obtained from the Hatch–Melbourne–Wübbena (HMW, Hatch Ron 1982; Melbourne 1985; Wübbena 1985) combination measurements.

Then, NL ambiguities are derived from the integer WL ambiguities and the estimated ionospheric-free (IF) ambiguities. The equations of EWL, WL and NL ambiguities are as follows:

$$\begin{aligned}\bar{N}^s_{r,\mathrm{ewl}\_jk} &= \left(\frac{L^s_{r,j}}{\lambda_j} - \frac{L^s_{r,k}}{\lambda_k} - \frac{(1-\alpha)P^s_{r,1} + \alpha P^s_{r,2}}{\lambda_{\mathrm{ewl}\_jk}}\right) \\ &= N^s_{r,\mathrm{ewl}\_jk} + d_{r,\mathrm{ewl}\_jk} - d^s_{\mathrm{ewl}\_jk}\end{aligned} \tag{3}$$

$$\begin{aligned}\bar{N}^s_{r,\mathrm{wl}\_ij} &= \left(\frac{L^s_{r,i}}{\lambda_i} - \frac{L^s_{r,j}}{\lambda_j} - \frac{(1-\beta)P^s_{r,1} + \beta P^s_{r,2}}{\lambda_{\mathrm{wl}\_ij}}\right) \\ &= N^s_{r,\mathrm{wl}\_ij} + d_{r,\mathrm{wl}\_ij} - d^s_{\mathrm{wl}\_ij}\end{aligned} \tag{4}$$

$$\begin{aligned}\lambda_{\mathrm{nl}\_ij}\cdot\bar{N}^s_{r,\mathrm{nl}\_ij} &= \lambda_{\mathrm{IF}\_ij}\cdot\bar{N}^s_{r,\mathrm{IF}\_ij} - \frac{cf_j}{f_i^2 - f_j^2}\cdot N^s_{r,\mathrm{wl}\_ij} \\ &= N^s_{r,\mathrm{nl}\_ij} + d_{r,\mathrm{nl}\_ij} - d^s_{\mathrm{nl}\_ij}\end{aligned} \tag{5}$$

with

$$\alpha = \frac{f_1^2 f_2^2 - f_2^2 f_j f_k}{f_j f_k\left(f_1^2 - f_2^2\right)} \tag{6}$$

$$\beta = \frac{f_1^2 f_2^2 - f_2^2 f_i f_j}{f_i f_j\left(f_1^2 - f_2^2\right)} \tag{7}$$

where $\bar{N}^s_{r,\mathrm{ewl}\_jk}$, $\bar{N}^s_{r,\mathrm{wl}\_ij}$ and $\bar{N}^s_{r,\mathrm{nl}\_ij}$ are float EWL, WL and NL ambiguities, respectively, while the N^s_{r,ewl_jk}, N^s_{r,wl_ij} and N^s_{r,nl_ij} are corresponding integer ambiguities, $\lambda_{\mathrm{ewl}\_jk}$ is the wavelength of the EWL ambiguity, which can be expressed as $\lambda_{\mathrm{ewl}\_jk} = \frac{c}{f_j - f_k}$, λ_{wl_ij} and λ_{nl_ij} denote wavelength of the WL and NL ambiguities, which can be written as $\lambda_{\mathrm{wl}\_ij} = \frac{c}{f_i - f_j}$ and $\lambda_{\mathrm{nl}\_ij} = \frac{c}{f_i + f_j}$, d_{r,ewl_jk},d_{r,wl_ij} and d_{r,nl_ij} denote EWL, WL and NL UPDs at the receiver, respectively, whereas $d^s_{\mathrm{ewl}\_jk}$, $d^s_{\mathrm{wl}\_ij}$ and $d^s_{\mathrm{nl}\_ij}$ denote the corresponding satellite UPDs. Based on the ambiguities from IGS tracking network, the EWL, WL and NL UPDs of Galileo satellites can be precisely estimated by least squares (Li and Zhang 2012; Li et al. 2013).

Since the Galileo satellites transmitted signals on five frequencies, there are ten types of HMW combinations with different wavelengths. The specific combinations, as well as their wavelength, are shown in Table 1. It can be seen that the HMW combinations wl_{23}, wl_{24}, wl_{25}, wl_{34}, wl_{35} and wl_{45} have obviously longer wavelengths than others. Thus, ambiguities of these six combinations are usually regarded as the EWL ambiguities in the Galileo PPP AR processing, while the others are considered as the WL ambiguities.

Table 1 HMW combinations of Galileo and the respective wavelength

Frequency combination	Wavelength (m)	Tag
E1/E5a	0.75	WL
E1/E5b	0.81	WL
E1/E5	0.78	WL
E1/E6	1.01	WL
E5a/E5b	9.77	EWL
E5a/E5	19.54	EWL
E5a/E6	2.93	EWL
E5b/E5	19.54	EWL
E5b/E6	4.19	EWL
E5/E6	3.45	EWL

Multi-frequency PPP AR model

With the precise UPD products, the extra-wide-lane, wide-lane and finally narrow-lane ambiguity can be fixed sequentially. Based on the combination observable (3) and (4), the float EWL and WL ambiguities can be obtained. Then the corresponding UPD products are applied to remove the satellite UPDs, and the receiver UPDs are calculated by averaging the fractional parts of all the available ambiguities. After the correction of the satellite and receiver UPDs, the EWL and WL ambiguities are fixed to integers according to the round strategy (Dong and Bock 1989).

Once the integer EWL and WL ambiguities are obtained, we developed an ambiguity-fixed ionospheric-free (AFIF) wide-lane measurement, which can be taken as a high-precision code measurement to enable rapid convergence for ambiguity-fixed solutions (Geng and Bock 2013). The AFIF wide-lane measurement P^s_{r,x_ijk} can be written as:

$$\begin{aligned}P^s_{r,x\_ijk} &= \frac{f_i}{f_i - f_k}L^s_{r,w\_ij} - \frac{f_k}{f_i - f_k}L^s_{r,e\_jk} \\ &- \lambda_{wl\_ij}\frac{f_i}{f_i - f_k}\left(N^s_{wl\_ij} + d_{r,wl\_ij} - d^s_{wl\_ij}\right)\end{aligned} \tag{8}$$

with

$$L^s_{r,w\_ij} = \frac{f_i}{f_i - f_j}L^s_{r,i} - \frac{f_j}{f_i - f_j}L^s_{r,j} \tag{9}$$

$$L^s_{r,e\_jk} = \frac{f_j}{f_j - f_k}L^s_{r,j} - \frac{f_k}{f_j - f_k}L^s_{r,k} - \lambda_{\mathrm{ewl}\_jk}\left(N^s_{r,\mathrm{ewl}\_jk} + d_{r,\mathrm{ewl}\_jk} - d^s_{\mathrm{ewl}\_jk}\right) \tag{10}$$

because of the long wavelengths of EWL and WL, the respective ambiguities can be fixed in a few epochs. The resultant AFIF observations can be taken as the high-precision code observations and used as the external constraint for PPP processing. With the assistance of the AFIF

observations, it is expected to speed up the convergence of NL ambiguities. To search for the optimal integer solution of the NL ambiguity, we use a search strategy based on LAMBDA (Teunissen 1995), and the ratio test is used to validate the ambiguity with a threshold of 2 (Han 1997).

Given observations on more frequencies, more types of AFIF observations can be formulated. In our study, P^s_{r,x_123}, P^s_{r,x_124}, P^s_{r,x_125}, P^s_{r,x_143} and P^s_{r,x_145} were employed for triple-frequency PPP AR based on E1/E5a/E5b, E1/E5a/E5, E1/E5a/E6, E1/E5/E5b and E1/E5/E6 frequencies, respectively. It is worth noting that the noise amplification factor of AFIF wide-lane measurement P^s_{r,x_125} and P^s_{r,x_145} is lower than P^s_{r,x_123}, P^s_{r,x_124} and P^s_{r,x_143}. Also, the measurements P^s_{r,x_124} and P^s_{r,x_143} have similar noise level as P^s_{r,x_123}. For quad-frequency (based on E1/E5a/E5b/E6 frequencies) and five-frequency (based on E1/E5a/E5b/E5/E6 frequencies) PPP AR, two and five types of AFIF measurement can be formulated, respectively. In the process of quad-frequency PPP ambiguity resolution, we use P^s_{r,x_123} and P^s_{r,x_125} together to achieve faster convergence. Furthermore, in order to utilize the observations from all available signals and achieve the best positioning performance, the measurement P^s_{r,x_123}, P^s_{r,x_125} and P^s_{r,x_145} can be used together to implement the five-frequency PPP AR.

Data and processing strategy

Data for a 10-day period sampled at 30 s from DOY 060 to 069 of 2019 are processed to estimate Galileo UPD products and evaluate the positioning performance of multi-frequency PPP AR. Figure 1 shows the distribution of the Galileo reference network. The 134 IGS stations are denoted by the blue triangles and are used for UPD estimation. The 18 user stations denoted by the red triangles are used to perform Galileo multi-frequency PPP AR. All these user stations can receive Galileo's five-frequency observations.

Currently, the Galileo constellation already consists of 26 satellites. The two satellites launched on August 22, 2014 (E14 and E18) missed their target and are in non-nominal elliptical orbits (Delva et al. 2015). Additionally, two other satellites, E20 and E22, are unserviceable (Steigenberger and Montenbruck 2017). Therefore, the present Galileo constellation consists of 22 properly functioning satellites, 2 testing satellites in improper orbits, and 2 unserviceable satellites (Hadas et al. 2019). The constellation has been completed in terms of numbers, although further launches will place back-up satellites in orbit in the future (https://www.gsa.europa.eu/galileo-initial-services).

To give a visual presentation of the geometry strength with Galileo constellation, Fig. 2 shows the average number of visible satellites on a global scale on DOY 062 of 2019, with the elevation cutoff of 10 degrees. From the figure, the visible satellites of Galileo are unequally distributed reaching in numbers from 4 to 10. The average number of visible satellites is 7.6. In most regions, more than 8 Galileo satellites can be tracked.

The data quality of Galileo signals on E1, E5a, E5b, E5 and E6 frequencies are analyzed in terms of multipath, noise and signal–noise ratio (SNR). The sum of multipath and noise can be described by a multipath combination (MP), which is as follows (Estey and Meertens 1999),

$$M_{P_i} = P_i - \frac{f_i^2 + f_j^2}{f_i^2 - f_j^2} L_i + \frac{2f_j^2}{f_i^2 - f_j^2} L_j \tag{11}$$

where M_{P_i} is code multipath combination. As for the frequency pairs of carrier phases corresponding to each MP combination, for the cases i: E5a, E5b, E5 and E6, we set j: E1, and for the case i: E1, we set j: E5 (Zaminpardaz and Teunissen 2017). The SNR is defined as the ratio of the

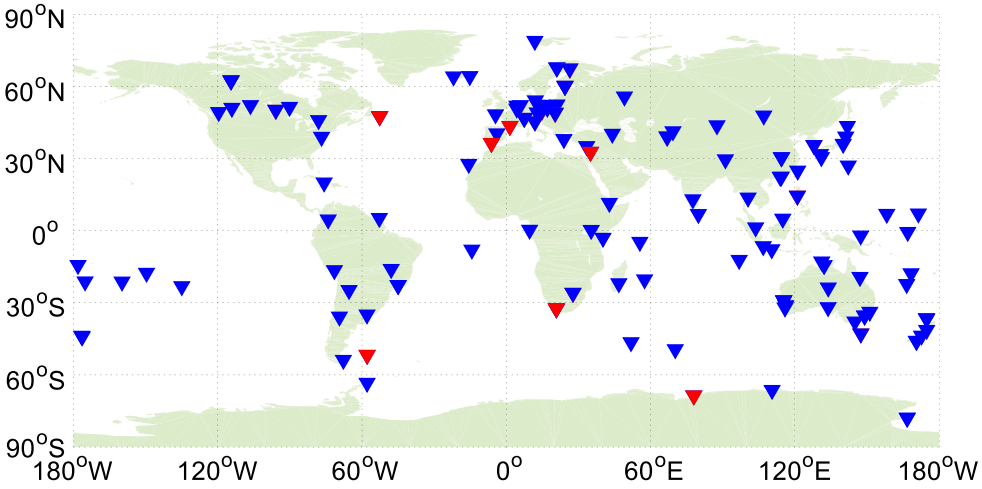

Fig. 1 Distribution of the Galileo reference network and user stations. The blue triangles denote the reference stations used for UPDs estimation, and the red triangles denote the user stations

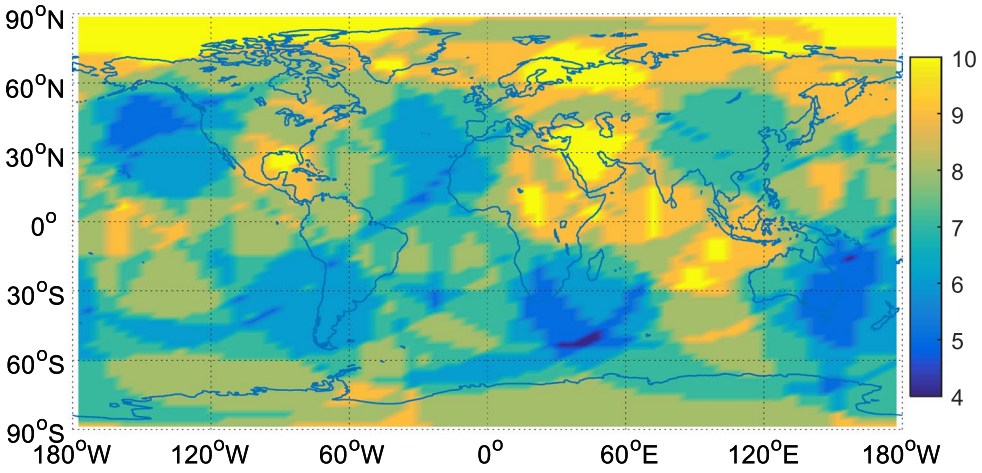

Fig. 2 Average number of visible satellites for Galileo constellation on DOY 062 of 2019. The elevation cutoff is 10 degree

received signal power to the received noise power, which provides an important indicator for the characterization of the received signals.

The MP combinations and SNR values for Galileo five-frequency signals at station MET3 on DOY 062 of 2019 are shown in Fig. 3. The top panel shows the MP combinations as a function of time on all frequencies for visible Galileo satellites. The magnitude of the MP combination on E5 frequency is within 0.3 m while that on E1/E5a/E5b/E6 frequencies is within 1 m. That is to say, the code multipath effect and the noise level of E5 signals show significantly smaller values than that of the other frequencies (Zaminpardaz and Teunissen 2017). The SNR values on five frequencies as the function of the elevation angles are shown in the bottom panel of Fig. 3. From the figure, we can clearly see that the SNR values are strongly dependent on the elevation angles. The higher the elevation angles are, the larger the SNR values. The E5 frequency signals show higher SNR values than other frequencies. From the results of our analysis, we can conclude that E5 frequency signals have the highest quality.

For the purpose of investigating the performance of triple-frequency PPP AR, three solutions, including triple-frequency PPP float solutions (TF-float), dual-frequency PPP fixed solutions (DF-fixed) and triple-frequency PPP fixed solutions (TF-fixed), are analyzed and compared. All dual-frequency PPP solutions are based on E1/E5a frequencies in this study. Triple-frequency PPP with five types of frequency combinations (including E1/E5a/E5b, E1/E5a/E5, E1/E5a/E6, E1/E5/E5b and E1/E5/E6 frequencies) is compared to explore the optimal triple-frequency combination. Moreover, to make use of Galileo five-frequency observations, quad-frequency PPP AR (QF-fixed) and five-frequency PPP AR (FF-fixed) are also developed and evaluated.

The positioning performance is assessed in terms of TTFF, convergence time and positioning accuracy. In this study, the TTFF is defined as the time taken for the first ambiguity to be successfully fixed and the ambiguity can be fixed correctly during three consecutive epochs. The convergence time denotes the time taken for the horizontal accuracy to be better than 5 cm and kept within 5 cm during ten consecutive epochs (Feng and Wang 2008; Li et al. 2018). To evaluate the performance of multi-frequency PPP WAR for achieving decimeter-level positioning, we define a convergence time (< 0.10 m) and (< 0.50 m) as the time taken for the horizontal accuracy to be better than 0.10/0.50 m and kept within 0.10/0.50 m during ten consecutive epochs, respectively. The positioning accuracy is assessed by comparing our PPP coordinates with reference coordinates from the network solutions with Position And Navigation Data Analyst (PANDA) software (Liu and Ge 2003).

Results

The temporal characteristics of the EWL, WL and NL UPDs are investigated first in this section. Thereafter, the positioning performance of multi-frequency PPP AR is analyzed in terms of TTFF, convergence time and positioning accuracy. With the EWL and WL ambiguities successfully fixed as part of the PPP ambiguity resolution, we also implement the instantaneous decimeter-level positioning.

UPD results

The UPDs, which destroy the integer nature of ambiguity, should be precisely estimated and then provided to users for ambiguity resolution. In this section, UPD results (including EWL, WL and NL UPDs) of Galileo satellites with five types of frequency combinations (including E1/E5a/E5b, E1/E5a/E5, E1/E5a/E6, E1/E5/E5b and E1/E5/E6 frequencies) are investigated.

The EWL and WL UPDs of Galileo satellites from DOY 060-069 of 2019 are shown in Figs. 4 and 5, respectively.

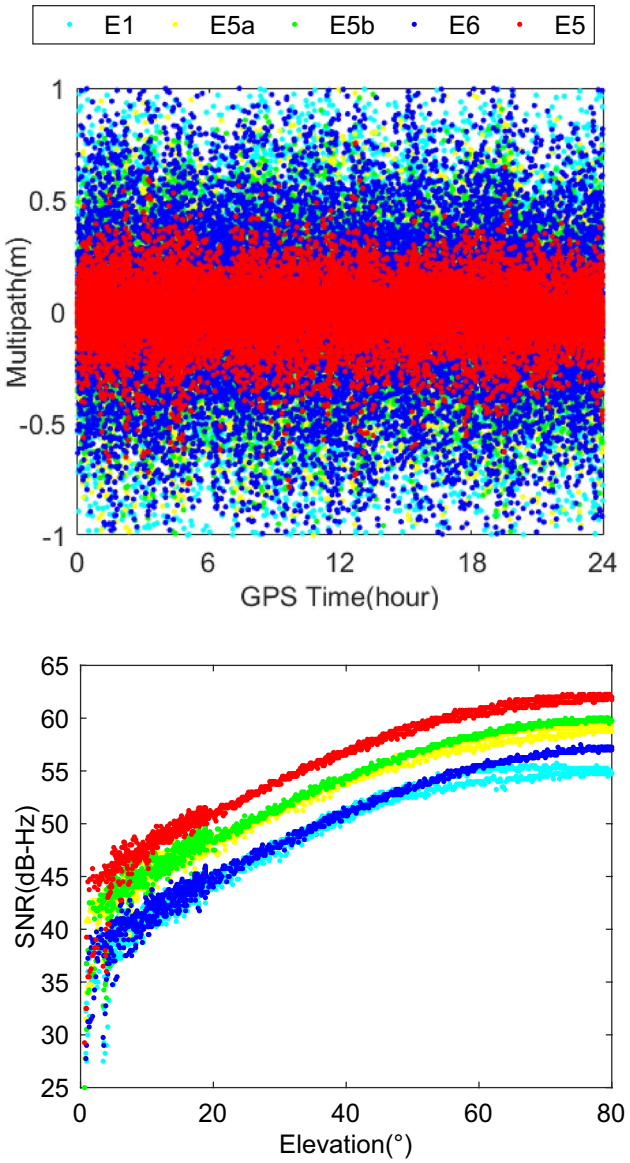

Fig. 3 Multipath combinations (top) and SNR values (bottom) for Galileo five-frequency signals at station MET3 on DOY 062 of 2019. E1 frequency (cyan), E5a frequency (yellow), E5b frequency (green), E6 frequency (blue), and E5 frequency (red)

Here E01 is selected as a reference. Benefiting from the high-quality observations and long wavelength of (extra-) wide-lane ambiguity, the EWL and WL UPD series are remarkably stable. From left to right (Fig. 4), the EWL UPDs on E5a/E5b, E5a/E5, E5a/E6, E5/E5b and E5/E6 combined frequencies are shown, respectively. It is interesting to find that the EWL UPDs on E5a/E5b, E5a/E5 and E5/E5b combined frequencies are very close to zero. This phenomenon may be associated with the characteristic of the alternative binary offset carrier (Alt-BOC) signals, which ensures a high correlation of code/phase delay of the signals on those three adjacent frequencies (Li et al. 2019). The WL UPDs on E1/E5a and E1/E5 combined frequencies are shown on the left and right panels of Fig. 5, respectively. The WL UPD values of these two frequency combinations present the high agreement, which further demonstrated that the phase biases of E5a and E5 signals are almost the same values. Figure 6 shows the daily NL UPDs (derived from five types of frequency combinations) on DOY 062 of 2019. The NL UPDs are relatively stable with no obvious fluctuation on the whole day. The NL UPDs derived from five types of frequency combinations agree well with each other.

Moreover, the standard deviations (STDs) of EWL, WL and NL UPDs are shown in top, middle and bottom panels of Fig. 7, respectively. The averaged STDs of Galileo EWL, WL and NL UPDs are presented in Table 2. The STDs of EWL and WL UPDs are within 0.015 cycles, and the EWL UPDs are more stable than the WL ones because of the longer wavelength. The STDs of NL UPDs are within 0.10 cycles and the averaged STDs of NL UPDs on E1/E5a/E5b, E1/E5a/E5, E1/E5a/E6, E1/E5/E5b and E1/E5/E6 frequencies are 0.034, 0.031, 0.029, 0.019 and 0.028 cycles, respectively. Due to the high-quality of E5 frequency signals, the stability of NL UPDs on E1/E5/E5b and E1/E5/E6 frequencies is slightly higher than other frequency combinations.

Galileo triple-frequency PPP AR

With the stable UPD products obtained, the triple-frequency PPP AR can be achieved. From left to right panels of Fig. 8, positioning errors of triple-frequency PPP solutions on E1/E5a/E5b, E1/E5a/E5, E1/E5a/E6, E1/E5/E5b and E1/E5/E6 frequencies are shown, respectively. Triple-frequency PPP float solutions, dual-frequency PPP fixed solutions and triple-frequency PPP fixed solutions are shown by green, blue and red lines, respectively. Compared to triple-frequency

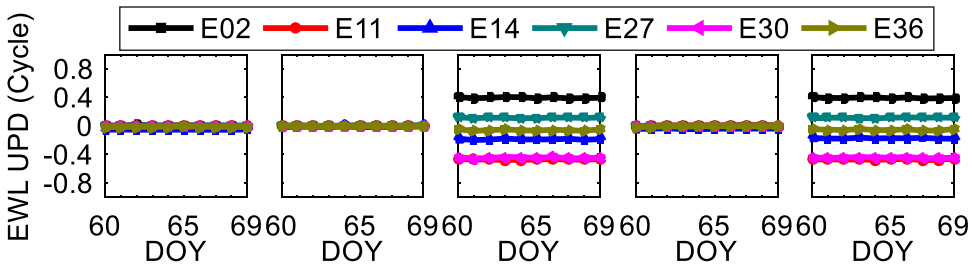

Fig. 4 EWL UPDs of Galileo satellites from DOY 060 to DOY 069 of 2019 (from left to right: E5a/E5b, E5a/E5, E5a/E6, E5/E5b and E5/E6 combined frequencies)

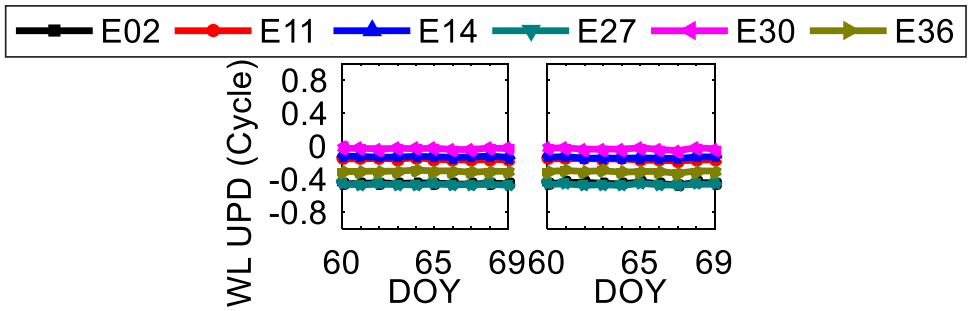

Fig. 5 WL UPDs of Galileo satellites from DOY 060 to DOY 069 of 2019 (from left to right: E1/E5a and E1/E5 combined frequencies)

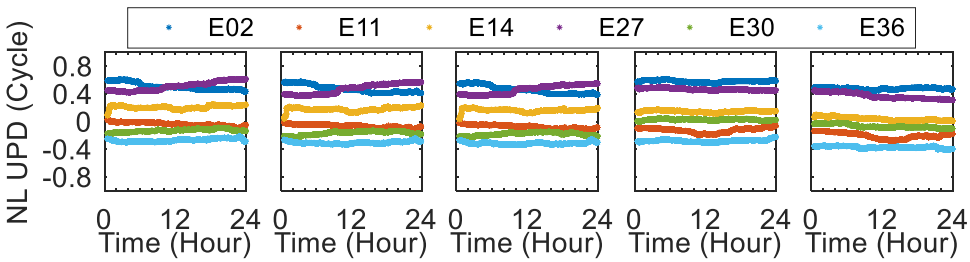

Fig. 6 NL UPDs of Galileo satellites on DOY 062 of 2019 (from left to right: E1/E5a/E5b, E1/E5a/E5, E1/E5a/E6, E1/E5/E5b and E1/E5/E6 frequencies)

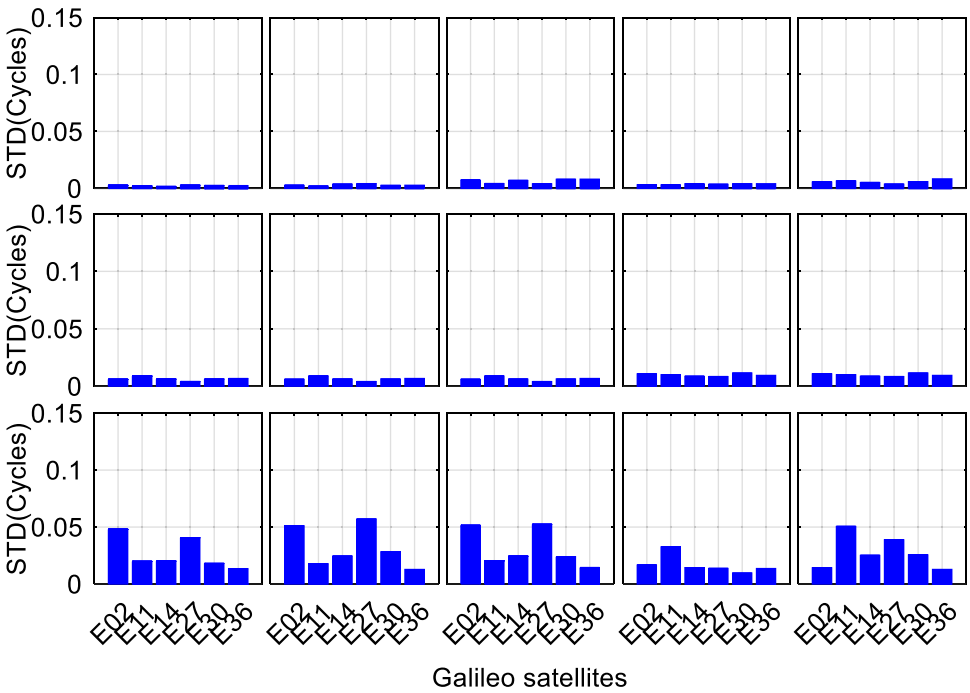

Fig. 7 STDs of EWL (top), WL (middle) and NL (bottom) UPDs of Galileo satellites (from left to right: E1/E5a/E5b, E1/E5a/E5, E1/E5a/E6, E1/E5/E5b and E1/E5/E6 frequencies)

Table 2 Averaged STDs of Galileo EWL, WL and NL UPDs (unit: cycles)

	E1/E5a/E5b	E1/E5a/E5	E1/E5a/E6	E1/E5/E5b	E1/E5/E6
EWL	0.002	0.003	0.006	0.003	0.005
WL	0.007	0.007	0.007	0.010	0.010
NL	0.034	0.031	0.029	0.019	0.028

PPP float solutions, positioning accuracy and convergence can be improved with the ambiguity fixed successfully. In addition, the triple-frequency PPP AR with five types of frequency combinations exhibits better positioning performance than dual-frequency PPP AR.

For the purpose of evaluating and comparing the performance of triple-frequency PPP AR with five types of

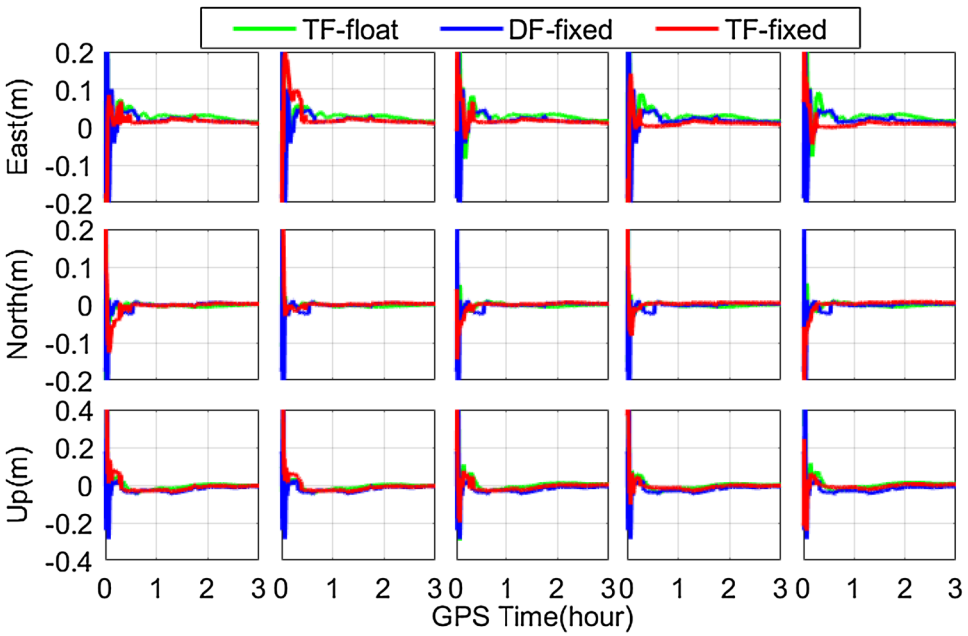

Fig. 8 Positioning errors of Galileo triple-frequency PPP solutions at station MET3 on DOY 062 of 2019 (from left to right: E1/E5a/E5b, E1/E5a/E5, E1/E5a/E6, E1/E5/E5b and E1/E5/E6 frequencies)

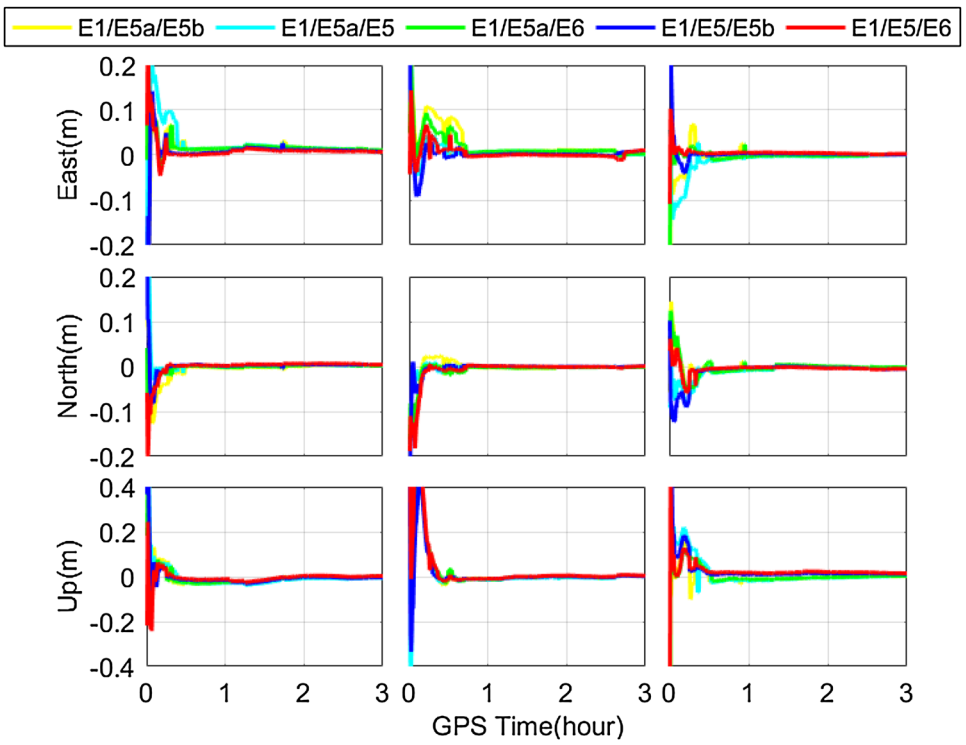

Fig. 9 Positioning errors of Galileo triple-frequency PPP AR at station MET3 (left), ROAG (middle), and STJ3 (right) on DOY 062 of 2019

frequency combinations, positioning errors at station MET3, ROAG and STJ3 on DOY 062 of 2019 are shown in Fig. 9. The triple-frequency PPP AR on E1/E5a/E5b, E1/E5a/E5, E1/E5a/E6, E1/E5/E5b and E1/E5/E6 frequencies are shown by yellow, cyan, green, blue and red lines, respectively. Obviously, during the initialization process, triple-frequency PPP AR on E1/E5/E6 frequencies show a more continuous and higher positioning accuracy compared with other frequency combinations.

Moreover, the averaged TTFF and convergence time for dual- and triple-frequency PPP AR is shown in Table 3. The averaged TTFF is 18.5-19.8 min for triple-frequency PPP AR, which is a slight improvement compared to dual-frequency PPP AR with 19.9 min of TTFF. However, the

Table 3 Averaged TTFF and convergence time of Galileo dual- and triple-frequency PPP AR (unit: min)

	DF-fixed	E1/E5a/E5b	E1/E5a/E5	E1/E5a/E6	E1/E5/E5b	E1/E5/E6
TTFF	19.9	18.8	19.8	19.4	18.7	18.5
Convergence time	22.3	17.4	21.6	18.9	18.3	16.9

averaged convergence time of triple-frequency PPP AR based on E1/E5a/E5b, E1/E5a/E5, E1/E5a/E6, E1/E5/E5b and E1/E5/E6 frequencies is 17.4, 21.6, 18.9, 18.3 and 16.9 min, which is an improvement of 22.0%, 3.1%, 15.2%, 17.9% and 24.2% compared to dual-frequency solutions, respectively. Among the five types of frequency combinations, the triple-frequency PPP AR on E1/E5/E6 shows the fastest convergence because of the high quality of E5 observations and the low noise amplification factor of the AFIF wide-lane combination.

Figure 10 presents the averaged positioning errors of 30-min Galileo triple-frequency PPP solutions with five types of frequency combinations, which are shown by yellow squares, cyan circles, green rhombuses, blue pentacles and red triangles, respectively. The Galileo triple-frequency PPP float solutions with 30-min observations can achieve an accuracy of less than 4 cm in the horizontal components and less than 6 cm in the vertical component. With the ambiguity resolution, the positioning accuracy of triple-frequency PPP AR can be significantly improved to less than 8 mm in the horizontal components and 1–3 cm in the vertical component. Moreover, compared to dual-frequency PPP AR with an accuracy of (1.1, 0.5, 2.2) cm in the east, north and up components, respectively, the triple-frequency PPP AR also show better performance. Taking Galileo PPP on E1/E5/E6 frequencies for example, triple-frequency PPP AR improves the positioning accuracy by 85.7%, 75.0% and 62.8% compared to triple-frequency float solutions, and 54.7%, 27.6% and 13.8% compared to dual-frequency PPP AR in the east, north and up components, respectively.

Galileo multi-frequency PPP AR

In this section, the triple-frequency (based on E1/E5/E6 frequencies), quad-frequency (based on E1/E5a/E5b/E6 frequencies) and five-frequency PPP AR is discussed, and the positioning performance is compared. Figure 11 shows the positioning errors of Galileo multi-frequency PPP AR at stations MET3, PTGG and SOD3 on DOY 062 of 2019. The dual-/triple-/quad-/five-frequency PPP fixed solutions are denoted by cyan, green, blue and red lines, respectively. Compared with dual-frequency PPP AR, triple-/quad-/five-frequency PPP AR can significantly shorten the convergence and improve the positioning accuracy. Moreover, the five-frequency PPP AR shows the best positioning performance.

The statistical TTFF and convergence time of Galileo multi-frequency PPP AR are further given in Table 4. Compared with TTFF of 19.9 min for dual-frequency PPP AR, the averaged TTFF can be slightly improved to 18.5 min, 18.5 min and 18.5 min for triple-/quad-/five-frequency PPP AR, respectively. Moreover, the averaged convergence time can be shortened to 15.3 min and 15.0 min for Galileo quad- and five-frequency PPP AR, which is an improvement of 31.4 and 32.7% compared to dual-frequency PPP AR, respectively. In comparison with triple-frequency PPP AR, the convergence time is improved by 9.5% and 11.2 for quad- and five-frequency PPP AR, respectively. Although the convergence time can be shortened to 15.0 min for Galileo multi-frequency PPP AR, it still takes about 20 min to achieve the ambiguity resolution of the narrow lane, which may be related to the long convergence time of atmospheric parameters.

Instantaneous decimeter-level positioning

The previous studies indicate that the Galileo multi-frequency PPP AR still requires about 20 min to fix the NL ambiguities. Fortunately, the EWL and WL ambiguities can be fixed to integers very quickly. It is expected that a high positioning accuracy can be achieved with the EWL and WL

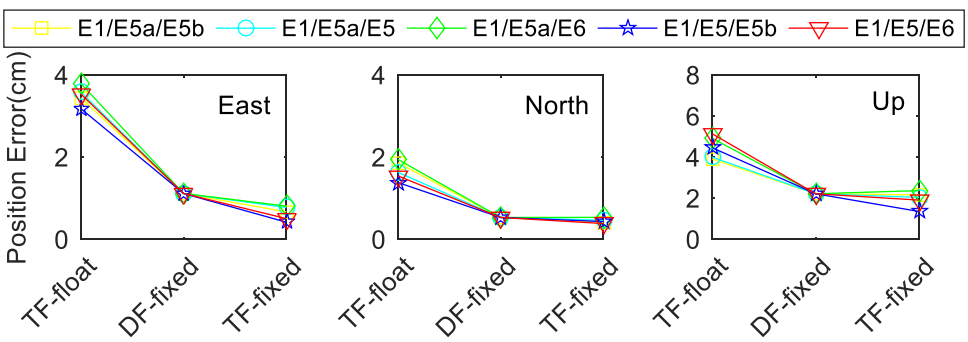

Fig. 10 Averaged positioning errors of 30-min Galileo PPP solutions

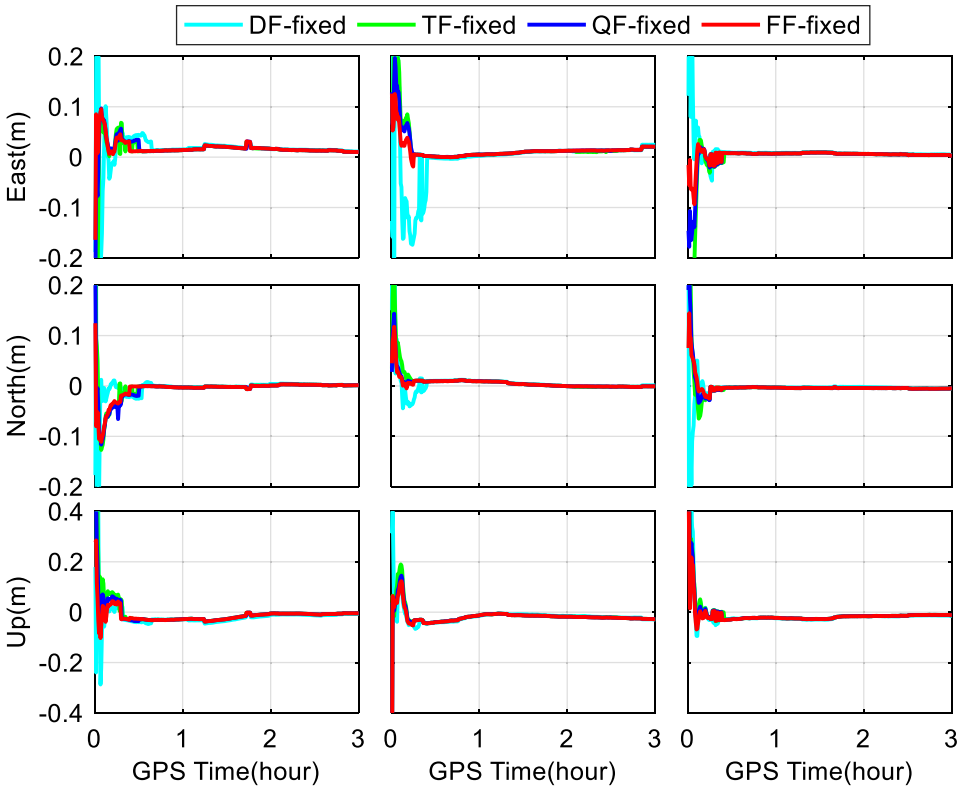

Fig. 11 Positioning errors of Galileo multi-frequency PPP AR at station MET3 (left), PTGG (middle) and SOD3 (right) on DOY 062 of 2019

ambiguity resolution. In this section, the results of Galileo PPP in triple-frequency PPP float solutions, triple-frequency wide-lane ambiguity resolution (TF-WAR), quad-frequency PPP wide-lane ambiguity resolution (QF-WAR) and five-frequency wide-lane ambiguity resolution (FF-WAR) are illustrated and compared.

Figure 12 shows the positioning errors of Galileo multi-frequency PPP WAR at station DAV1 on DOY 062 of 2019. Triple-frequency PPP float solutions, triple-, quad- and five-frequency PPP WAR are shown by cyan, green, blue and red lines, respectively. Compared to float solutions, the positioning accuracy of multi-frequency PPP WAR converges to decimeter-level instantaneously, especially in the horizontal components. As expected, as observations on more frequencies are used, the better performance can be achieved.

Success rate of first-epoch fixing is defined as the percentage of ambiguities that are fixed to correct integers over all ambiguities at the first epoch. The success rate of the EWL and WL ambiguities is 98.5% and 87.1%, respectively. In most cases, the EWL and WL ambiguities can be fixed instantaneously. We further calculated the positioning errors of the first epoch for Galileo multi-frequency solutions, and the averaged positioning errors are given in Table 5. For triple-/quad-/five-frequency PPP WAR with single-epoch observations, decimeter-level positioning can be achieved in horizontal components. The positioning accuracy of Galileo five-frequency PPP WAR is (0.112, 0.144, 0.641) m, which is an improvement of 42.0%, 36.6% and 22.7% compared to triple-frequency PPP WAR, and 17.0%, 16.8% and 2.1% compared to quad-frequency PPP WAR in the east, north and up components, respectively.

Furthermore, the averaged convergence time of Galileo multi-frequency PPP WAR is shown in Table 6. The notation <0.50 m and <0.10 m denotes the time for the horizontal accuracy is better than 0.50/0.10 m and kept within 0.50/0.10 m during ten consecutive epochs, respectively. Instantaneous decimeter-level positioning can be achieved for Galileo triple-/quad-/five-frequency PPP WAR, and the averaged convergence time (<0.50 m) is 0.5 min, 0.2 min and 0.2 min, respectively, while triple-frequency PPP float solution takes 3.4 min to achieve decimeter-level positioning. With single-epoch observations, PPP WAR can achieve better positioning performance compared with PPP float solutions.

Table 4 Averaged TTFF and convergence time of Galileo multi-frequency PPP AR (unit: min)

	DF-fixed	TF-fixed	QF-fixed	FF-fixed
TTFF	19.9	18.5	18.5	18.5
Convergence time	22.3	16.9	15.3	15.0

Conclusion

We developed a multi-frequency PPP AR method to make use of the Galileo five-frequency observations. The multi-frequency UPD products were estimated first, and then the

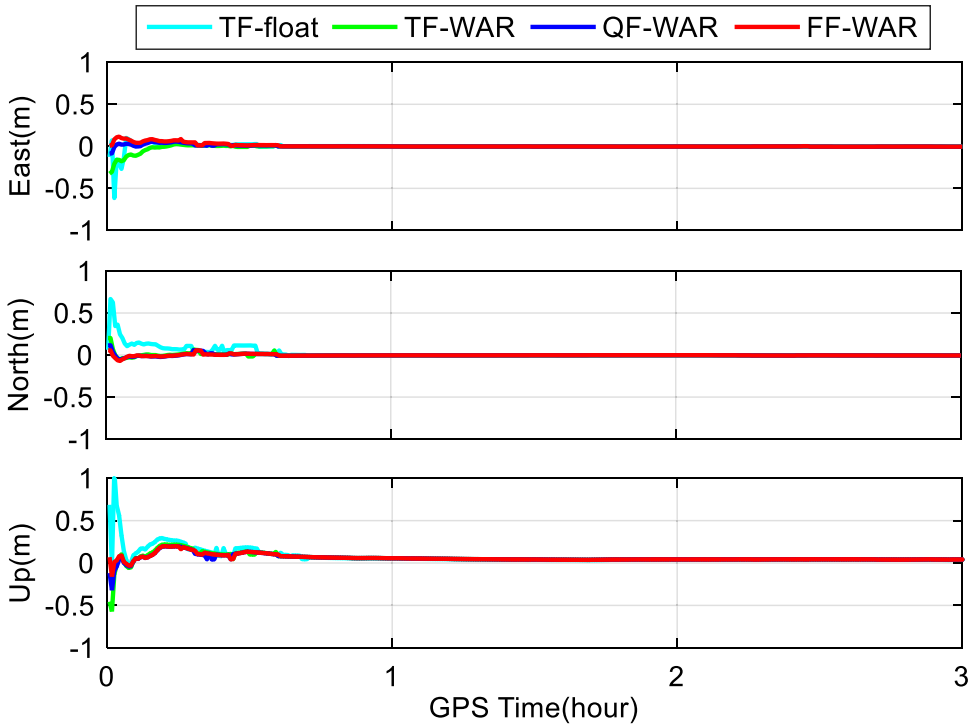

Fig. 12 Positioning errors of Galileo multi-frequency PPP WAR at station DAV1 on DOY 062 of 2019

Table 5 Averaged positioning errors of first epoch Galileo multi-frequency PPP WAR (unit: m)

	East	North	Up
TF-WAR	0.193	0.227	0.829
QF-WAR	0.135	0.173	0.655
FF-WAR	0.112	0.144	0.641

Table 6 Averaged convergence time of Galileo multi-frequency PPP WAR (unit: min)

	TF-float	TF-WAR	QF-WAR	FF-WAR
< 0.50 m	3.4	0.5	0.2	0.2
< 0.10 m	15.2	16.0	6.2	6.0

triple-, quad- and five-frequency PPP AR were carried out. The performance of triple-frequency PPP AR with five types of frequency combinations (including E1/E5a/E5b, E1/E5a/E5, E1/E5a/E6, E1/E5/E5b and E1/E5/E6 frequencies) was assessed and compared to find the optimal combination. Moreover, the contribution of quad- and five-frequency observations to PPP AR was also evaluated.

Observations of 134 stations acquired from the IGS network from DOY 060 to 069 of 2019 are used for Galileo UPD estimation. The EWL and WL UPD series of Galileo satellites are remarkably stable with the STDs less than 0.015 cycles, and the NL UPDs are relatively stable in the whole day with all STDs within 0.10 cycles. It is interesting to find that the EWL UPDs on E5a/E5b, E5a/E5 and E5/E5b combined frequencies are very close to zero, which may be related to Alt-BOC modulation of Galileo E5 signals. Moreover, with high quality of E5 frequency observations, the stability of NL UPDs derived from E1/E5/E5b and E1/E5/E6 PPP solutions is higher than other frequency combinations.

With high-quality UPD products, Galileo triple-/quad-/five-frequency PPP AR can be achieved. The performance of PPP solutions was evaluated in terms of TTFF, convergence time, and positioning accuracy. Triple-frequency PPP AR improves the positioning accuracy by 36.6–86.8% compared to triple-frequency PPP float solutions for 30-min PPP solutions. In addition, the triple-frequency PPP AR also exhibits better performance than dual-frequency PPP AR, and the positioning accuracy is improved by 2.3–62.5%. Compared with the averaged convergence time of 22.3 min for dual-frequency PPP AR, 16.9–21.6 min can be achieved for triple-frequency PPP AR, which is an improvement of 3.1–24.2%. The triple-frequency PPP AR on E1/E5/E6 frequencies show the fastest convergence of 16.9 min among five types of frequency combinations, due to the high quality of observations and the low noise amplification factor of AFIF wide-lane measurements. The averaged convergence time of quad- and five-frequency PPP AR can be further shortened to 15.3 min and 15.0 min from 22.3 min, respectively. However, the averaged TTFF of multi-frequency PPP NL AR is 18.5–19.8 min, which is only shortened by about 1 min compared to dual-frequency PPP AR (19.9 min). This phenomenon may be related to the fact that atmospheric parameters still require a long time to converge.

Fortunately, the EWL and WL ambiguities can be fixed to integers very quickly. Our results indicate that the success rate of first-epoch fixing for the EWL and WL ambiguities is 98.5 and 87.1%, respectively. With the EWL and WL ambiguities fixed successfully, instantaneous decimeter-level positioning can be achieved for Galileo triple-/quad-/five-frequency PPP WAR. The positioning accuracy of the first epoch for Galileo five-frequency PPP WAR is (0.112, 0.144, 0.641) m in the east, north and up components, respectively, which is an improvement of 2.1–42.0% compared to triple- and quad-frequency PPP WAR. The convergence time (< 0.50 m) of triple-/quad-/five-frequency PPP WAR is 0.5 min, 0.2 min and 0.2 min, respectively, while it is 3.4 min for triple-frequency PPP float solutions. From our analysis in this study, we can conclude that multi-frequency observations bring a significant improvement in convergence and instantaneous positioning capability of PPP AR.

Acknowledgements This work has been supported by Key Laboratory of Geospace Environment and Geodesy, Ministry of Education, Wuhan University:18-02-09, the National Natural Science Foundation of China under Grant 41774030, Grant 41974027, and Grant 41974029, in part by the Hubei Province Natural Science Foundation of China under Grant 2018CFA081.

References

Cai C, He C, Santerre R, Pan L, Cui X, Zhu J (2016) A comparative analysis of measurement noise and multipath for four constellations: GPS, BeiDou, GLONASS and Galileo. Surv Rev 48(349):287–295

Collins P, Lahaye F, Herous P, Bisnath S (2008) Precise point positioning with AR using the decoupled clock model. In: Proceedings of the ION GNSS 2008, Savannah, GA, USA, 16–19 Sept, pp 1315–1322

Delva P, Puchades N, Schönemann E, Dilssner F, Courde C, Bertone S, Gonzalez F, Hees A, Le Poncin-Laftte Ch, Meynadier F (2015) A gravitational redshift test using eccentric Galileo satellites. Phys Rev Lett 121(23):231101. https://doi.org/10.1103/PhysRevLett.121.231101

Deo M, El-Mowafy A (2016) Triple-frequency GNSS models for PPP with float ambiguity estimation: performance comparison using GPS. Surv Rev 50(360):249–261

Dong D, Bock Y (1989) Global positioning system network analysis with phase ambiguity resolution applied to crustal deformation studies in California. J Geophys Res 94(B4):3949–3966

Estey LH, Meerten CM (1999) TEQC: the multi-purpose toolkit for GPS/GLONASS data. GPS Solut 3(1):42–49

Feng Y, Wang J (2008) GPS RTK performance characteristics and analysis. J Glob Pos Syst 7(1):1–8

Geng J, Bock Y (2013) Triple-frequency GPS precise point positioning with rapid ambiguity resolution. J Geod 87(5):449–460

Gu S, Lou Y, Shi C, Liu J (2015) Beidou phase bias estimation and its application in precise point positioning with triple-frequency observable. J Geod 89(10):979–992

Hadas T, Kazmierski Kamil, Sośnica Krzysztof (2019) Performance of Galileo-only dual-frequency absolute positioning using the fully serviceable Galileo constellation. GPS Solut 4(23):108. https://doi.org/10.1007/s10291-019-0900-9

Han S (1997) Quality-control issues relating to instantaneous ambiguity resolution for real-time GPS kinematic positioning. J Geod 71(6):351–361

Hatch R (1982) The synergism of GPS code and carrier measurements. In: Proceedings of the third international symposium on satellite doppler positioning at physical sciences laboratory of New Mexico State University, 8–12 Feb, vol 2, pp 1213–1231

Henkel P, Gunther C (2008) Precise point positioning with multiple galileo frequencies. In: Proceedings of IEEE/ION PLANS 2008, Monterey, CA, May, pp 592–599

Kouba J (2009) A guide to using international GNSS service (IGS) products. http://igscb.jpl.nasa.gov/igscb/resource/pubs/UsingIGSProductsVer21.pdf

Li X, Zhang X (2012) Improving the estimation of uncalibrated fractional phase offsets for PPP ambiguity resolution. J Navig 65(3):513–529

Li X, Ge M, Zhang H, Wickert J (2013) A method for improving uncalibrated phase delay estimation and ambiguity-fixing in real-time precise point positioning. J Geod 87(5):405–416

Li X, Ge M, Dai X, Ren X, Fritsche M, Wickert J, Schuh H (2015) Accuracy and reliability of multi-GNSS real-time precise positioning: GPS, GLONASS, BeiDou, and Galileo. J Geod 89(6):607–635

Li X, Li X, Yuan Y, Zhang K, Zhang X, Wickert J (2018) Multi-GNSS phase delay estimation and PPP ambiguity resolution: GPS, BDS, GLONASS, Galileo. J Geod 92:579–608. https://doi.org/10.1007/s00190-017-1081-3

Li X, Li X, Liu G, Feng G, Yuan Y, Zhang K, Ren X (2019) Triple-frequency PPP ambiguity resolution with multi-constellation GNSS: BDS and Galileo. J Geod. https://doi.org/10.1007/s00190-019-01229-x

Liu J, Ge M (2003) PANDA software and its preliminary result of positioning and orbit determination. J Nat Sci Wuhan Univ 8(2B):603–609. https://doi.org/10.1007/BF02899825

Malys S, Jensen PA (1990) Geodetic point positioning with gps carrier beat phase data from the CASA UNO experiment. Geophys Res Lett 17(5):651–654

Melbourne WG (1985) The case for ranging in GPS-based geodetic systems. In: Proceedings of the first international symposium on precise positioning with the global positioning system, Rockville, MD, USA, 5–19 April

Montenbruck O, Hauschild A, Steigenberger P, Hugentobler U, Teunissen P, Nakamura S (2013) Initial assessment of the COMPASS/BeiDou-2 regional navigation satellite system. GPS Solut 17(2):211–222. https://doi.org/10.1007/s10291-012-0272-x

Pan L, Zhang X, Li X, Liu J, Xin Li (2017) Characteristics of inter-frequency clock bias for Block IIF satellites and its effect on triple-frequency GPS precise point positioning. GPS Solut 21(2):811–822

Steigenberger P, Montenbruck O (2017) Galileo status: orbits, clocks, and positioning. GPS Solut 21(2):319–331

Teunissen PJG (1995) The least-squares ambiguity decorrelation adjustment: a method for fast GPS integer ambiguity estimation. J Geod 70(1–2):65–82

Wang K, Khodabandeh A, Teunissen P (2018) Five-frequency Galileo long baseline ambiguity resolution with multipath mitigation. GPS Solut 22(3):75

Wübbena G (1985) Software developments for geodetic positioning with GPS using TI-4100 code and carrier measurements. In: Proceedings of the first international symposium on precise positioning with the global positioning system, Rockville, MD, 5–19 April

Zaminpardaz S, Teunissen PJG (2017) Analysis of Galileo IOV + FOC signals and E5 RTK performance. GPS Solut 21(4):1855–1870

Zhang X, Li P, Guo F (2013) Ambiguity resolution in precise point positioning with hourly data for global single receiver. Adv Space Res 51(1):153–161

Zumberge JF, Heflin MB, Jefferson DC, Watkins MM, Webb FH (1997) Precise point positioning for the efficient and robust analysis of GPS data from large networks. J Geophys Res 102(B3):5005–5017

Publisher's Note Springer Nature remains neutral with regard to jurisdictional claims in published maps and institutional affiliations.

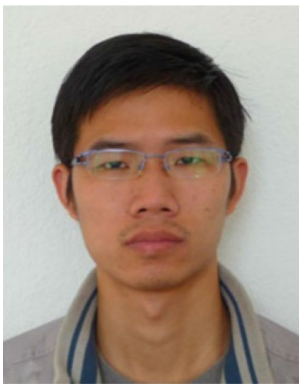

Xingxing Li is currently a professor at Wuhan University. He has completed his B.Sc. degree at the School of Geodesy and Geomatics at Wuhan University. He obtained his Ph.D. degree at the Department of Geodesy and Remote Sensing of the German Research Centre for Geosciences (GFZ). His current research mainly involves GNSS precise data processing and its application for geosciences.

Gege Liu is currently a Master candidate at Wuhan University. She has completed her B.Sc. at the School of Geodesy and Geomatics at Wuhan University in 2018. Her area of research currently focuses on multi-GNSS PPP ambiguity resolution.

Xin Li is currently a Ph.D. candidate at Wuhan University. She has completed her B.Sc. at the School of Geodesy and Geomatics at Wuhan University in 2015. Her area of research currently focuses on multi-GNSS PPP ambiguity resolution.

Feng Zhou is currently a lecturer at Shandong University of Science and Technology. He received his Ph.D. degree at the East China Normal University in 2018. His current research mainly focuses on multi-constellation and multi-frequency GNSS PPP.

Guolong Feng is currently a Master candidate at Wuhan University. He has completed his B.Sc. at the School of Geodesy and Geomatics in Wuhan University in 2018. His area of research currently focuses on GNSS meteorology.

Yongqiang Yuan is currently a Ph.D. candidate at Wuhan University. He has completed his B.Sc. at the School of Geodesy and Geomatics in Wuhan University in 2016. His area of research currently focuses on GNSS precise orbit determination.

Keke Zhang is currently a Ph.D. candidate at Wuhan University. He has completed his B.Sc. at the School of Geodesy and Geomatics in Wuhan University in 2016. His area of research currently focuses on GNSS precise orbit determination.